Carcinogenesis vol.34 no.9 pp.2080–2089, 2013
doi:10.1093/carcin/bgt169
Advance Access publication May 20, 2013

The antipsychotic agent chlorpromazine induces autophagic cell death by inhibiting the Akt/mTOR pathway in human U-87MG glioma cells

Soon Young Shin[1,2], Kyoung Sun Lee[3], Yang-Kyu Choi[3], Hyunjung Jade Lim[1], Hong Ghi Lee[4], Yoongho Lim[5] and Young Han Lee[1,2,*]

[1]Department of Biological Sciences, College of Biological Science and Biotechnology, Research Center for Transcription Control, Konkuk University, Seoul 143-701, Republic of Korea, [2]SMART Institute of Advanced Biomedical Science, Research Institute of Medical Science, Konkuk University Medical Center, Seoul 143-729, Republic of Korea, [3]Department of Laboratory Animal Medicine, College of Veterinary Medicine, Konkuk University, Seoul 143-701, Republic of Korea, [4]Department of Hematology, Konkuk University Hospital, Seoul 143-729, Republic of Korea and [5]Division of Bioscience and Biotechnology, BMIC, Konkuk University, Seoul 143-701, Republic of Korea

*To whom correspondence should be addressed. Tel: +82 2 2049 6115; Fax: +82 2 3437 9781;
Email: yhlee58@konkuk.ac.kr
Correspondence may also be addressed to Soon Young Shin.
Tel: +82 2 2030 7945; Fax: +82 2 3437 9781;
Email: shinsy@konkuk.ac.kr

2-Chloro-10-[3(-dimethylamino)propyl]phenothiazine mono hydrochloride (chlorpromazine; CPZ) is an antipsychotic agent that was originally developed to control psychotic disorders. The cytotoxic properties of the CPZ are well known, but its mechanism of action is poorly understood. In this study, we investigated the role of apoptosis and autophagy in CPZ-induced cytotoxicity in U-87MG glioma cells. CPZ treatment inhibited cell proliferation and long-term clonogenic survival. Additionally, CPZ triggered autophagy, as indicated by electron microscopy and accumulation of the membrane form of microtubule-associated protein 1 light chain 3 (LC3-II); however, CPZ did not induce apoptosis. Inhibition of autophagy by expression of Beclin 1 small interfering RNA (siRNA) in U-87MG cells attenuated CPZ-induced LC3-II formation. Furthermore, U-87MG cells expressing Beclin 1 siRNA attenuated CPZ-induced cell death. CPZ inhibited phosphatidylinositol 3-kinase (PI3K)/AKT/ mTOR pathway in U-87MG cells. Treatment with LY294002, a PI3K inhibitor, alone increased the accumulation of LC3-II and potentiated the effect of CPZ. In contrast, exogenous expression of AKT partially inhibited CPZ-induced LC3-II formation. When U-87MG cells were implanted into the brain of athymic nude mouse, CPZ triggered autophagy and inhibited xenograft tumor growth. These results provided the first evidence that CPZ-induced cytotoxicity is mediated through autophagic cell death in PTEN (phosphatase and tensin homolog deleted on chromosome 10)-null U-87MG glioma cells by inhibiting PI3K/AKT/mTOR pathway.

Introduction

Autophagy is an evolutionally conserved and a self-destructive process, which is induced by various stimuli, including nutrient depletion and genotoxic stress (1). Autophagy functions as the elimination of intracellular parasites, harmful aggregated proteins and excess or damaged organelles within characteristic vacuoles known as the autophagosome, which is fused with lysosome to become the autolysosome.

Abbreviations: ATG, autophagy-related gene; BrdU, bromodeoxyuridine; CaM, calmodulin; CPZ, chlorpromazine; DMEM, Dulbecco's modified Eagle's medium; EM, electron microscopy; GAPDH, glyceraldehyde 3-phosphate dehydrogenase; GFP, green fluorescent protein; LC3, microtubule-associated protein 1 light chain 3; mTOR, mammalian target of rapamycin; PARP, poly(ADP-ribose) polymerase; PBS, phosphate-buffered saline; PI, propidium iodide; PI3K, phosphatidylinositol 3-kinase; PTEN, phosphatase and tensin homolog; siRNA, small interfering RNA.

Autophagy is essential for a long-term survival mechanism when cells suffer nutrient starvation. Inhibition of autophagy results in rapid cell death under conditions of starvation or withdrawal of growth factors (2). In some cancer cells, autophagy is induced by chemotherapy or radiotherapy and may protect cells undergoing apoptosis (programmed type-I cell death), resulting in unfavorable conditions after anticancer therapy (2). In contrast, several studies have reported that autophagy triggers apoptosis-independent cell death in response to various anticancer agents, including sodium trioxide, tamoxifen, temozolomide, nelfinavir (3) and plumbagin (4). Thus, autophagy is also implicated in promoting cellular suicide (programmed type-II cell death), presumably due to irreversible massive self-destruction of cellular contents or activation of death signal pathways (5). In human glioma cells, autophagy provides a protective mechanism of cancer cells against radiotherapy and chemotherapy (6–9); in contrast, some anticancer agents, including minocycline, oncolytic adenovirus, α-mangostin and curcumin, have been reported to induce autophagic cell death (10–13). Whether autophagy provides survival or induction of cell death in glioma cells remains controversial.

Phosphatidylinositol 3-kinase (PI3K) is an enzyme that is activated by diverse signaling agents, including platelet-derived growth factor, epidermal growth factor and insulin-like growth factor-1. It phosphorylates $PI(4,5)P_2$ to generate $PI(3,4,5)P_3$, resulting in the functional activation of Akt (protein kinase B). Activated Akt phosphorylates a series of protein substrates that function as a regulator of cell proliferation, growth and cell survival. PI3K/Akt signaling is commonly hyperactivated in various cancer types and often confers a poor prognosis (14,15). PTEN (phosphatase and tensin homolog deleted on chromosome 10), also known as MMAC1 (mutated in multiple advanced cancer) or TEP1 (TGFβ-regulated and epithelial cell-enriched phosphatase), is a lipid phosphatase that removes the 3′-phosphate group from $PI(3,4,5)P_3$ and converts it to $PI(4,5)P_2$, thereby negatively regulating the PI3K/Akt signal pathway. Loss of PTEN activity is known to be caused by chromosomal gene mutation, epigenetic silencing due to DNA methylation in the promoter region of the gene or aberrant proteolytic events, which is responsible for the deregulated activation of PI3K/Akt signaling (16). Accumulating evidence has suggested that the PI3K/Akt pathway plays an important role in the regulation of autophagy (17,18). Indeed, the PI3K inhibitor LY294002 and Akt inhibitor 7-hydroxystaurosporine synergistically augment rapamycin-induced autophagy (19) and inhibition of the PI3K/Akt pathway by curcumin exposure induces non-apoptotic autophagic cell death in PTEN-null U-87MG malignant glioma cells (13).

2-Chloro-10-[3(-dimethylamino) propyl] phenothiazine monohydrochloride (chlorpromazine; CPZ) is a phenothiazine derivative belonging to the first generation of a typical antipsychotic agent. In addition to dopamine receptor antagonistic activity (20), CPZ may bind to several proteins, including calmodulin (CaM), several channel proteins, DNA topoisomerase, oncogenic K-Ras and other membrane proteins (21,22). CPZ shows beneficial effects on the antiproliferation of various tumor cells (23,24), probably through inhibition of the mitotic kinesin KSP/Eg5 that results in mitotic arrest (25), upregulation of $p21^{Waf1/Cip1}$ expression via activation of tumor-suppressor Egr-1 or through inhibition of the 3-phosphoinosite-dependent protein kinase 1/Akt signaling pathway (26). However, whether CPZ stimulates autophagy in human glioma cells is still unknown.

The aim of this study was to obtain insight into the action of CPZ in the regulation of autophagy and the functional role of autophagy on tumor cell growth in PTEN-null U-87MG glioma cells. To establish this, we analyzed cell cycle control, long-term clonogenic survival, apoptosis and autophagy following CPZ treatment. We found that CPZ induces apoptosis-independent autophagic cell death and inhibits clonogenicity of U-87MG cells *in vitro* and xenografted tumor growth

© The Author 2013. Published by Oxford University Press. All rights reserved. For Permissions, please email: journals.permissions@oup.com

Downloaded from https://academic.oup.com/carcin/article/34/9/2080/2463384 by guest on 20 August 2022

in vivo. We also investigated the signal pathways responsible for CPZ-induced autophagy and found that CPZ inhibits the AKT/mTOR pathway. These results provide additional mechanistic insight into CPZ-induced non-apoptotic autophagic cell death and further support CPZ as an attractive therapeutic adjuvant for treatment of PTEN-null or AKT-hyperactivated human gliomas.

Materials and methods

Reagents

CPZ was purchased from Sigma-RBI (Natick, MA). Antibodies specific to poly(ADP-ribose) polymerase (PARP) were obtained from Cell Signaling Technology (Beverly, MA). The antibodies for cyclin D1, proliferating cell nuclear antigen, cyclin A, cyclin B1, Beclin 1, Atg5, microtubule-associated protein 1 light chain 3 (LC3) and glyceraldehyde 3-phosphate dehydrogenase (GAPDH) were obtained from Santa Cruz Biotechnology (Santa Cruz, CA). The Alexa Fluor 558-conjugated secondary antibody was obtained from Invitrogen (Carlsbad, CA). Expression plasmid for AKT (pSG5/Akt) was a generous gift from Julian Downward (Cancer Research UK London Research Institute, UK).

Cell culture

U-87MG human glioma cells were obtained from the American Type Culture Collection (Rockville, MD) and maintained in Dulbecco's modified Eagle's medium (DMEM) containing 10% fetal bovine serum, at 37°C in a 5% CO_2 atmosphere.

Cell viability and cell proliferation assay

U-87MG cells (2×10^3 cells per sample) seeded into 96 well plates were treated with CPZ at increasing concentrations (0, 10, 20 and 40 μM) for different time periods (0, 24 and 48 h). For cell viability, a Cell Counting Kit-8™ (Dojindo Molecular Technologies) was used, according to the manufacturer's instructions. For cellular proliferation, cells were labeled with bromodeoxyuridine (BrdU) for 2 h, and the incorporation of BrdU was measured using an ELISA Cell Proliferation Assay Kit (Cell Signaling Technology), according to the manufacturer's instructions.

Cell death analysis

At indicated time points, U-87MG cells were trypsinized and washed in phosphate-buffered saline (PBS), and treated with 2.5 μg/ml propidium iodide (PI) for 5 min at room temperature. For quantification of dead cells, PI-stained cells were analyzed using a FACSCalibur flow cytometer (Becton Dickinson Immunocytometry Systems, San Jose, CA).

Clonogenic survival assay

U-87MG cells (5×10^3 cells per well) were counted and plated onto 24 well tissue culture plates (BD Falcon™; Becton Dickson Immunocytometry System) in DMEM supplemented with 10% fetal bovine serum. After attachment, the cells were treated with CPZ for 7 days. The cells were then fixed with 6% glutaraldehyde and stained with 0.1% crystal violet, as described previously (27).

Cell cycle analysis

U-87MG cells were treated with 20 μM CPZ for 12 and 24 h, fixed in 70% ethanol, washed twice with PBS and stained with 50 μg/ml PI, as described previously (28). The cellular DNA content was analyzed, and the population in the sub-G_0/G_1 phase of the cell cycle was measured by flow cytometry in a FACSCalibur.

Western blot analysis

Cells were lysed in a buffer containing 20 mM hydroxyethyl piperazineethanesulfonic acid (pH 7.2), 1% Triton X-100, 10% glycerol, 150 mM NaCl, 10 μg/ml leupeptin and 1 mM phenylmethylsulfonyl fluoride. Western blotting was performed as described previously (28). Signals were developed using an enhanced chemiluminescence detection system (Amersham Pharmacia Biotech, Piscataway, NJ).

Apoptosis assay using Annexin V

U-87MG cells (1×10^6 cells per sample) were treated with CPZ (10, 20 or 40 μM) or doxorubicin (1 μg/ml) as a positive control for 24 h, and cells were fixed and incubated with Cy3-conjugated Annexin V (BD Pharmingen, San Diego, CA), according to the manufacturer's instructions. Fluorescence-positive cells were analyzed by flow cytometry in a FACSCalibur instrument.

Electron microscopy

U-87MG cells either left untreated or treated with CPZ for 24 h were fixed with a solution of 2.5% glutaraldehyde in 0.1M phosphate buffer (pH 7.4) for 2 h and postfixed with 1% phosphate-buffered osmium tetroxide for 1 h. They were then dehydrated using a graded series of ethanol solutions ranging from 30 to 100%, transferred to propylene oxide and embedded in Epon (Polybed 812; Polysciences, Warrington, PA), as described previously (29). Ultrathin sections were prepared using an ultramicrotome (Leica Microsystems, Bannockburn, IL) and stained with 2% uranylacetate in 50% methanol and lead citrate. They were finally examined using an H-7650 transmission electron microscope (Hitachi, Tokyo, Japan) at an accelerating voltage of 80 kV.

Green fluorescent protein-LC3 localization using fluorescence microscope

The expression plasmid for green fluorescent protein (GFP)-tagged LC3 was kindly provided by Dr Seung-Jae Lee (Department of Biomedical Science and Technology, Konkuk University, Seoul, Korea). U-87MG cells were seeded into 12 well plates and transfected with 0.5 μg of the GFP-LC3 plasmid using Lipofectamine 2000 reagent (Invitrogen Life Technologies, San Diego, CA), according to the manufacturer's instructions. At 24 h posttransfection, cells were treated with 20 μM CPZ for 24 h, fixed with 4% paraformaldehyde and examined under an EVOSf1® fluorescence microscope (Advance Microscopy Group, Bothell, WA). For detection of endogenous LC3, U-87MG cells were treated with 20 μM CPZ for 12 h, fixed and incubated with anti-LC3 antibody for 90 min and then Alexa Fluor 555-conjugated secondary antibody for 30 min. Nuclear DNA was stained with Hoechst 33258. Stained cells were immediately observed under an EVOSf1® fluorescence microscope (Advance Microscopy Group).

Generation of U-87MG variant cells stably expressing Beclin 1 small interfering RNA

U-87MG cells were transduced with MISSION® small hairpin RNA lentiviral particles expressing scrambled small interfering RNA (siRNA) or Beclin 1 siRNA (Sigma–Aldrich, St Louis, MO), according to the manufacturer's instructions. Twenty-four hours postinfection, 2 μg/ml of puromycin was added to select for infected cells. After 2 weeks, silencing of Beclin 1 expression was verified by western blotting.

In vivo tumor xenograft study

Xenograft tumor experiments were performed as described previously (30). Briefly, for the subcutaneous xenograft tumor model, U-87MG glioma cells (1×10^6 cells in 100 μl of serum-free DMEM) were inoculated subcutaneously into the right flank of 5- to 6-week-old athymic nude mice (Korea Research Institute of Bioscience and Biotechnology, Daejeon, Korea). Tumor growth was measured at intervals of every 2–3 days with calipers. The tumor volume was calculated as $(L \times W^2)/2$, where L is the length and W is the width in millimeters. When the tumors reached a mean volume of ~100 mm^3, 100 μl of PBS (control group) or CPZ (20 mg/kg) was injected intraperitoneally daily. Mice were killed by exposure to CO_2 on day 24 to compare the tumor size on cutaneous xenograft tumors.

For the intracranial xenograft tumor model, the mice were anesthetized with zoletil (30 mg/kg; Virbac Laboratories, Carros, France) and xylazine (5 mg/kg; Bayer Korea, Anseong, Korea). The surgical area over the parieto-occipital bone was applied with disinfectant, and an ~1 cm long sagittal incision was made using a scalpel. A 0.9 mm burr hole was drilled into the skulls at 2.0 mm to the right of the bregma and 1.0 mm anterior to the coronal suture, and U-87MG cells (1×10^5 cells in 10 μl of serum-free DMEM) were inoculated using a 10 μl Hamilton syringe, followed by covering the hole in sterile bone wax. After 4 days, PBS (control group) or CPZ (20 mg/kg) was injected intraperitoneally daily for 7 days. All mouse studies were performed at the veterinary facilities of Konkuk University in accordance with the Institutional Animal Care and Use Committee of Konkuk University.

Immunohistochemical analysis

Immunohistochemistry was performed using Vectastain *Elite* ABC Kits (Vector Laboratories, Burlingame, CA). LC3b monoclonal antibody (1:100; Abcam Corp., Cambridge, UK) was used as the primary antibody. Briefly, paraffin sections were deparaffinized, hydrated and heated in 0.01M sodium citrate for 10 min in a microwave to retrieve antigen. The sections were treated with 3% hydrogen peroxide in methanol and incubated with 5% bovine serum albumin. The brain sections were then incubated with the primary antibody overnight at 4°C. After washing in PBS, the sections were incubated with biotinylated secondary antibodies for 60 min and with avidin-biotin peroxidase complex for 30 min at room temperature. The sections were visualized with peroxidase substrate kits (Vector Laboratories) for immune reactivity, counterstained with hematoxylin and dehydrated in ethanol.

Statistical analysis

Each experiment was repeated at least three times. The data were plotted as the mean ± SD. Two-tailed Student's *t*-test was used for comparisons, and a value of $P < 0.05$ was deemed to be statistically significant.

Downloaded from https://academic.oup.com/carcin/article/34/9/2080/2463384 by guest on 20 August 2022

Results

CPZ promotes antitumoral action through induction of cell death

We first assessed the effectiveness of CPZ (Figure 1A) as a therapeutic agent in human gliomas. Exponentially growing PTEN-null U-87MG glioma cells were exposed to different concentrations of CPZ, and cellular proliferation was tested based on the incorporation of BrdU during DNA synthesis. A decrease in cellular proliferation was observed in cells treated with CPZ in a dose- and time-dependent manner compared with untreated control cells (Figure 1B, top graph). Cell viability was determined to examine the cytotoxic effects of CPZ using a Cell Counting Kit-8™. A significant decrease in cell viability was observed in cells treated for 24 h with high concentration of CPZ (≥20 μM) compared with untreated control cells (Figure 1B, bottom graph), probably due to the promotion of cell death. To address whether CPZ causes cell death, U-87MG cells were treated with CPZ for 24 h and stained with PI, which is an intercalating agent that can be used for identifying dead cells in a population. Flow cytometric analysis showed that CPZ caused cell death in a dose-dependent fashion (Figure 1C). The clonogenic (or colony forming) assay is based on the ability of a single cell to grow into a viable colony and is considered to be a reliable test for predicting the effectiveness of cytotoxic agents. To assess the long-term efficacy of CPZ, the clonogenic survival assay was performed. Significant decreases in the number of colonies were observed for U-87MG glioma cells after treatment with CPZ (Figure 1D). These results demonstrated that CPZ exhibits antitumor activity through induction of cell death.

CPZ triggers cell cycle arrest at the G_2/M phase and apoptosis-independent cell death

To determine whether the antitumor activity of CPZ is associated with inhibition of cell cycle progression, the cell cycle distribution profile was analyzed using flow cytometric analysis. Cells in the G_0/G_1 phase slowly decreased with a concomitant increase in G_2/M phase cells after treatment with CPZ (Figure 2A). Notably, accumulation of sub-G_1 phase cells, a hallmark of apoptosis, was not detected until 24 h after CPZ treatment. We next examined the effects of CPZ on the expression of cell cycle regulatory proteins. Immunoblot analysis showed that after 12 h of CPZ exposure, the levels of cyclin A and cyclin B1 decreased, whereas levels of cyclin D1, proliferating cell nuclear antigen and GAPDH remained unchanged (Figure 2B), suggesting that CPZ causes inhibition of cell cycle progression.

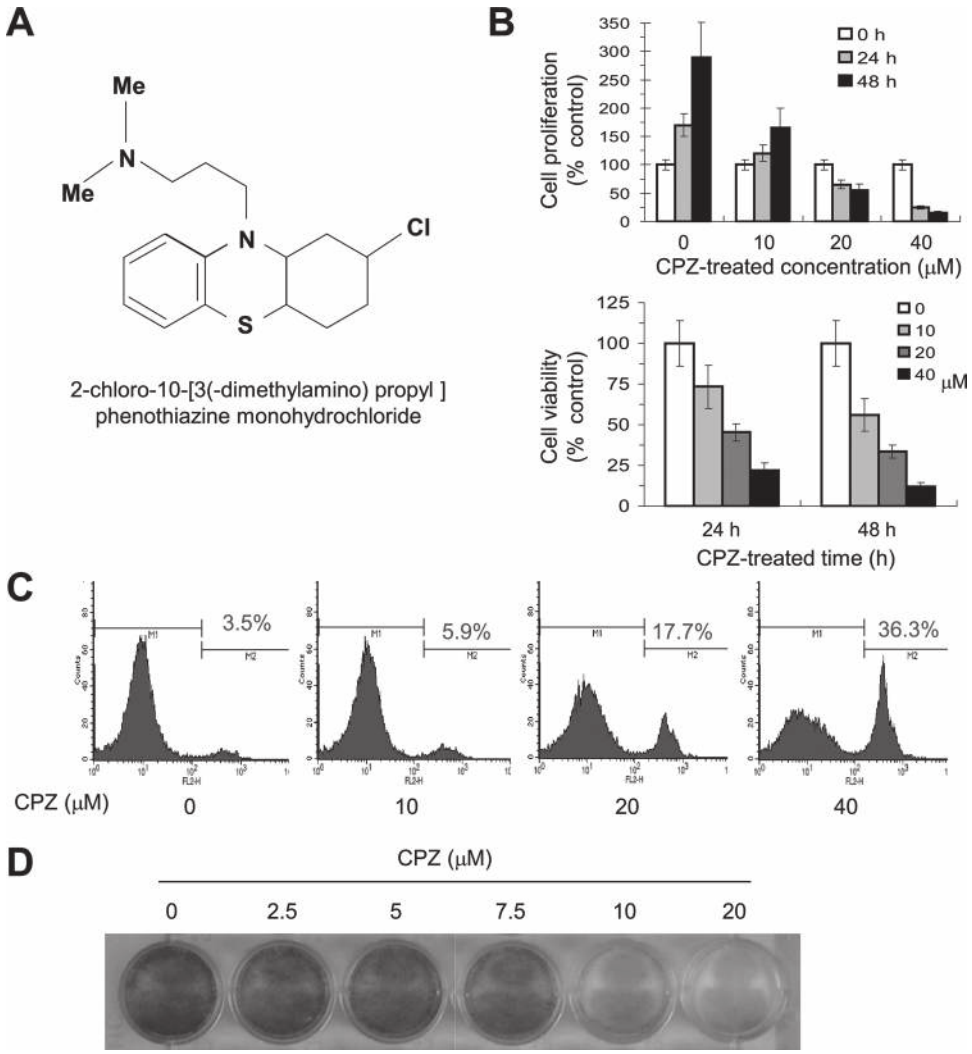

Fig. 1. Antitumor effects of CPZ in U-87MG glioma cells. (**A**) Chemical structure of CPZ. (**B**) U-87MG cells (1×10^3 cells per sample) were treated with different concentrations (0, 10, 20 and 40 μM) of CPZ for 24 or 48 h. Cell proliferation was examined using an ELISA Colorimetric Kit for the detection of BrdU incorporation (top graph) and cell viability was measured using a Cell Counting Kit-8 (bottom graph). Data represent the mean ± SD for two independent experiments performed in triplicate. (**C**) Cell death analysis by PI staining. U-87MG cells were treated with 10, 20 or 40 μM CPZ for 24 h, stained with 2.5 μg/ml PI for 5 min; PI-positive cells (dead cells) were assessed by flow cytometry. (**D**) Clonogenic survival assay. U-87MG cells (5×10^3) were seeded and cultured in the absence or presence of different concentrations of CPZ (0, 2.5, 5, 7.5 and 10 μM). After 7 days of treatment, colonies were stained with crystal violet.

Downloaded from https://academic.oup.com/carcin/article/34/9/2080/2463384 by guest on 20 August 2022

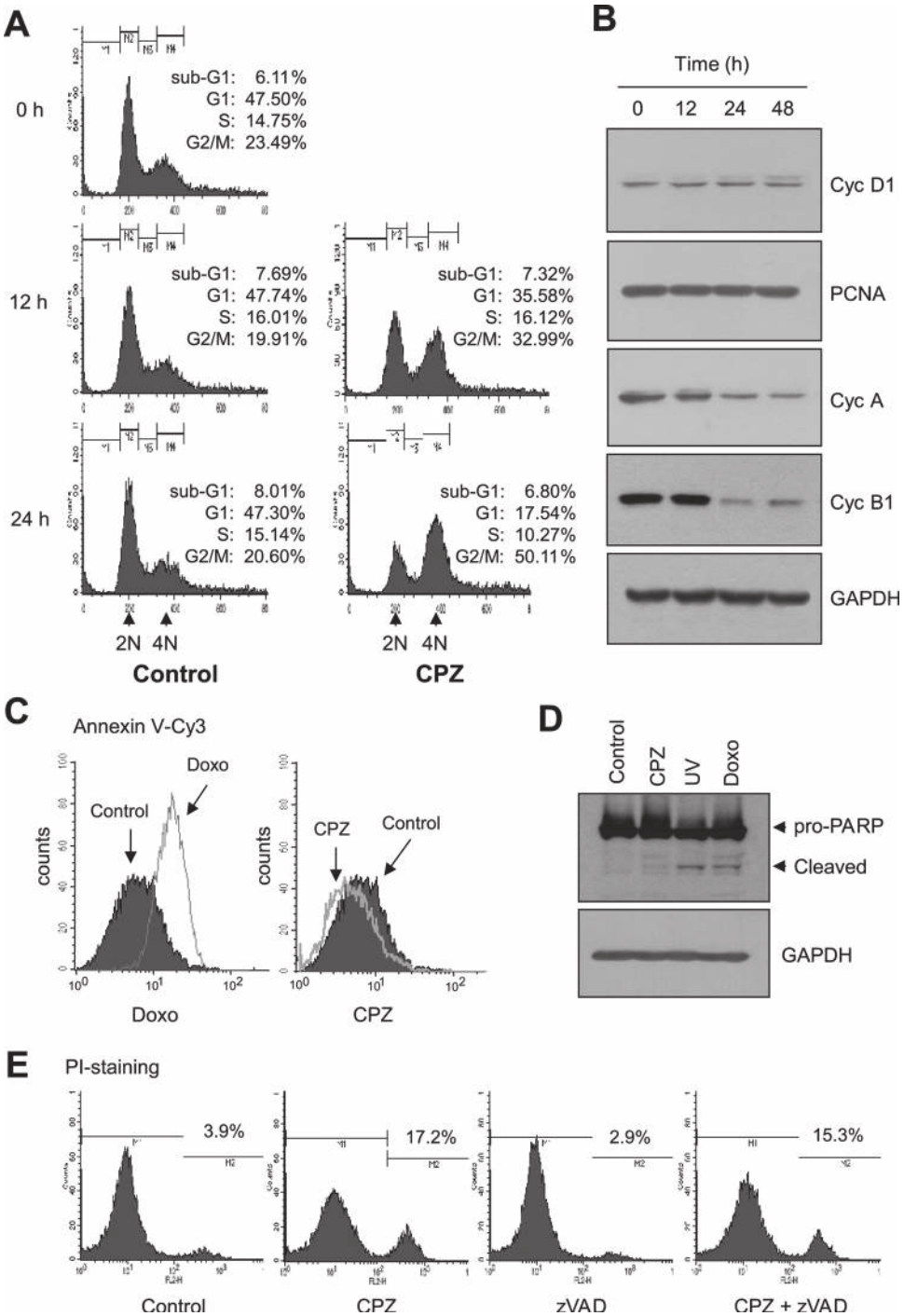

Fig. 2. Effects of CPZ on cell cycle arrest and cell death. (**A**) Fluorescence-activated cell sorting analysis. U-87MG cells (1×10^5 cells per sample) were treated with 20 μM CPZ for 12 or 24 h. Cells were harvested, fixed with ethanol and stained with PI. The cellular DNA content was then determined by flow cytometry. 2N, diploid; 4N, tetraploid; M1, sub-G_1 phase; M2, G_1 phase; M3, S phase; M4, G_2/M phase. (**B**) Western blot analysis. U-87MG cells were treated with 20 μM CPZ for various lengths of time, and whole-cell lysates were then subjected to western blotting using antibodies against the indicated proteins. GAPDH antibody was used as an internal control to show equal protein loading. (**C**) Apoptosis assay by Annexin V staining. U-87MG cells were stained with Annexin V-Cy3 after treatment with vehicle or 20 μM CPZ for 24 h. Doxorubicin (1 μg/ml) was used as a positive control. Cy3-positive cells (apoptotic cells) were analyzed by flow cytometry. (**D**) PARP cleavage analysis by western blotting. U-87MG cells were treated with 20 μM CPZ, 20 J/m^2 ultraviolet C (UVC) radiation, 1 μg/ml doxorubicin (Doxo) for 24 h; whole-cell lysates were then subjected to western blotting using antibody against PARP. GAPDH antibody was used as an internal control to show equal protein loading. (**E**) Cell death analysis. U-87MG cells were treated with 20 μM CPZ, 20 μM zVAD or CPZ plus zVAD for 24 h, and stained with PI, and PI-positive cells (dead cells) were assessed by flow cytometry.

As a flow cytometric analysis failed to reveal accumulation of cells in the sub-G_0/G_1 phase following CPZ treatment, we further examined the effect of CPZ on the induction of apoptosis. One of the earliest cellular changes during apoptosis is the translocation of phosphatidylserine (PS), a membrane phospholipid, from the inner to the outer membrane (31). To determine the appearance of PS at the outer membrane following CPZ treatment, Annexin V staining was performed. Doxorubicin was used as a positive control. We found no sign of PS translocation to the outer membrane in U-87MG cells treated with CPZ compared with that in control cells (Figure 2C).

Downloaded from https://academic.oup.com/carcin/article/34/9/2080/2463384 by guest on 20 August 2022

The processing of native 113 kDa PARP to its 89- and 24 kDa forms by caspase-3 or -7 can be induced in the early stage of apoptosis. However, treatment with CPZ for 24 h failed to cleave PARP, whereas ultraviolet irradiation or doxorubicin treatment for 24 h, used as positive controls for apoptosis, caused cleavage of PARP (Figure 2D). Furthermore, the pan-caspase inhibitor zVAD-fmk had no effect on CPZ-induced cell death (Figure 2E). These data suggest that CPZ may trigger cell death through apoptosis-independent mechanism in U-87MG cells.

CPZ induces autophagy

Two forms of programmed cell death exist; type-I (apoptosis) and type-II (autophagic cell death). Because CPZ treatment did not display typical apoptotic features, we next asked whether CPZ induces cell death through autophagy in U-87MG cells. Transmission electron microscopy (EM) revealed that CPZ treatment resulted in the appearance of numerous vacuoles, containing cellular fragments, whereas the nucleus maintained its integrity (Figure 3A), manifesting the typical feature of autophagy.

During autophagy, the18 kDa LC3-I protein is known to be cleaved to 16 kDa and conjugated to phosphatidylethanolamine (2) to form LC3-II, which is localized on the autophagosome membrane (32,33). LC3-I exhibits a diffuse staining pattern within the cytoplasm, whereas LC3-II is visualized in small puncta corresponding to the autophagosome (33). To verify the formation of the autophagosome by CPZ, we transiently transfected U-87MG cells with the expression plasmid for GFP-LC3. GFP-LC3-transfected cells showed a diffuse distribution of green fluorescence in the absence of CPZ (Figure 3B). In contrast, CPZ triggered the formation of punctated structures of GFP-LC3. We next determined the localization of endogenous LC3 using immunofluorescence staining. Similar to exogenous GFP-LC3, endogenous LC3 displayed the formation of a punctated fluorescent pattern in response to CPZ treatment (Figure 3C), representing an association of LC3-II with the autophagosome.

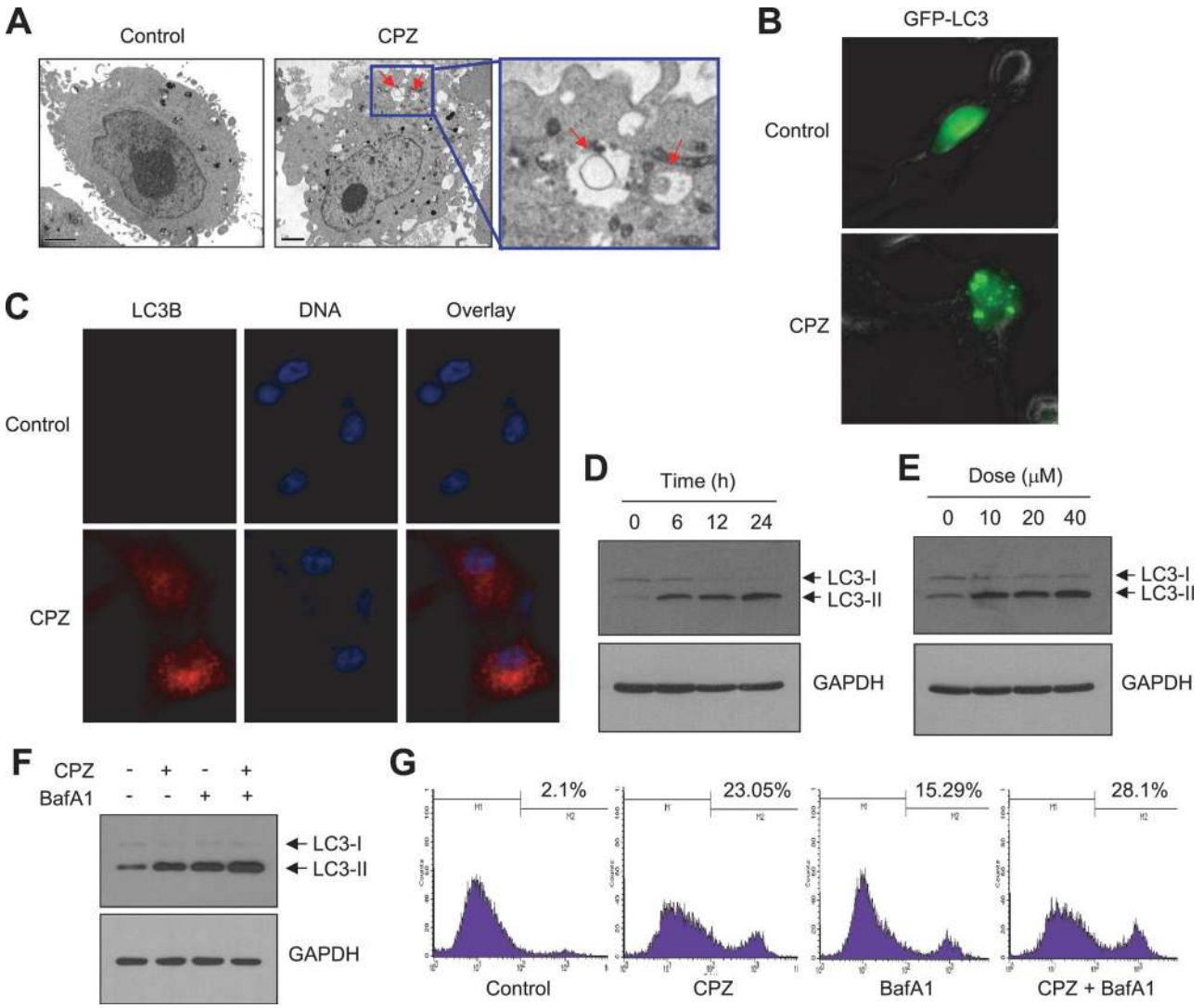

Fig. 3. Effect of CPZ on autophagy. (**A**) EM analysis. U-87MG cells were treated with 20 μM CPZ for 24 h and then analyzed by EM. Scale bars: 2 μm. (**B**) U-87MG cells transfected with an expression plasmid for GFP-LC3 were treated with 20 μM CPZ for 24 h. (**C**) U-87MG cells were treated with 20 μM CPZ for 12 h. LC3 (green signal) was stained through incubation with an LC3b antibody for 90 min and then Alexa Fluor 555-conjugated secondary antibody for 30 min. Nuclear DNA (blue signal) was stained with Hoechst 33258. Stained cells were observed under an EVOSf1® fluorescence microscope. (**D** and **E**) U-87MG cells were treated with 20 μM CPZ for different time periods (0, 6, 12 or 24 h) (D) or with different concentrations of CPZ (10, 20 or 40 μM) for 24 h (E), and whole-cell lysates were then subjected to western blotting using antibody against LC3b. GAPDH antibody was used as an internal control to show equal protein loading. (**F**) U-87MG cells were treated with 10 nM bafilomycin A1 (BafA1) for 30 min, followed by 20 μM CPZ for 24 h. Western blotting was performed as in (E). (**G**) U-87MG cells were treated with 10 nM BafA1 and 20 μM CPZ for 24 h as in (F) and then stained with 2.5 μg/ml PI for 5 min. PI-positive (dead) cells were assessed by flow cytometry.

Downloaded from https://academic.oup.com/carcin/article/34/9/2080/2463384 by guest on 20 August 2022

As the amount of LC3-II is correlated with the extent of autophagic vesicle formation, conversion of LC3-I to LC3-II serves as a hallmark for accumulation of the autophagosome and autophagic activity (33). To determine whether CPZ increases LC3-II formation in U-87MG cells, western blot analysis was performed using an antibody against LC3. CPZ treatment resulted in an increase in the amount of LC3-II in a time- and dose-dependent manner (Figure 3D and E). LC3-II accumulation can result from either the enhancement or inhibition of ongoing autophagic flux. To discriminate between these possibilities, bafilomycin A1, a vacuolar H^+-ATPase inhibitor, was used to prevent autophagosome-lysosome fusion. Treatment with bafilomycin A1 alone led to an increase in the amount of LC3-II, and the addition of CPZ to cells pretreated with bafilomycin A1 further increased the LC3-II level (Figure 3F), suggesting that CPZ enhances autophagic flux. As bafilomycin A1 alone triggered cell death (Figure 3G), we suggest that the prolonged inhibition of ongoing autophagic flux may promote cell death in U-87MG cells. Collectively, our results suggest that CPZ induces autophagy, probably by promoting autophagic vesicle formation, in U-87MG glioma cells.

Beclin 1 is required for CPZ-induced autophagy

Autophagy is controlled by a series of autophagy-related genes (ATGs). We examined whether CPZ alters the expression of ATG proteins. Western blot analysis showed that the protein levels of ATGs, except for LC3-II, did not change in response to CPZ treatment (Supplementary Figure 1, available at *Carcinogenesis* Online). Beclin 1, a mammalian ortholog of yeast Atg6/Vps30, is part of the class III PI3K multiprotein complex that participates in autophagosome nucleation (18,34–36). To investigate whether Beclin 1 is required for CPZ-induced autophagy in U-87MG cells, we established stable cell lines expressing Beclin 1 siRNA (U-87/siBECN1) and negative control siRNA (U-87/siCT). Knockdown of Beclin 1 expression was evaluated by western blotting. We found that CPZ-induced LC3-II accumulation was markedly reduced in U-87/siBECN1 cells compared with U-87/siCT cells (Figure 4A), suggesting that CPZ-induced autophagy requires Beclin 1-mediated pathway.

To advance our understanding of the role of CPZ induction of autophagy, we evaluated the consequence of disrupting autophagy in CPZ-induced antitumor activity. Knockdown of Beclin 1 had no effect on CPZ-induced G_2/M cell cycle arrest (Figure 4B), suggesting that the induction of autophagy and cell cycle arrest in response to CPZ might be controlled by distinct mechanisms. In contrast, lack of Beclin 1 expression led to an abrogation of CPZ-induced cell death (Figure 4C). To further address the role of autophagy, we knocked down another autophagy-related protein, ATG5. ATG5 is involved in LC3-II conjugation to phosphatidylethanolamine, which is necessary for the elongation of autophagic vesicles. We found that CPZ-induced LC3-II accumulation and cell death were attenuated by the knock down of ATG5 (Supplementary Figure 2, available at *Carcinogenesis* Online). These results underscore the impact of autophagy on CPZ-induced cell death. Collectively, our studies suggest that induction of autophagy by CPZ may function to contribute to CPZ-triggered cell death in U-87MG glioma cells. Furthermore, CPZ had no effect on the cleavage of PARP, but it induced LC3-II formation (Supplementary Figure 3A, available at *Carcinogenesis* Online) and reduced cell viability (Supplementary

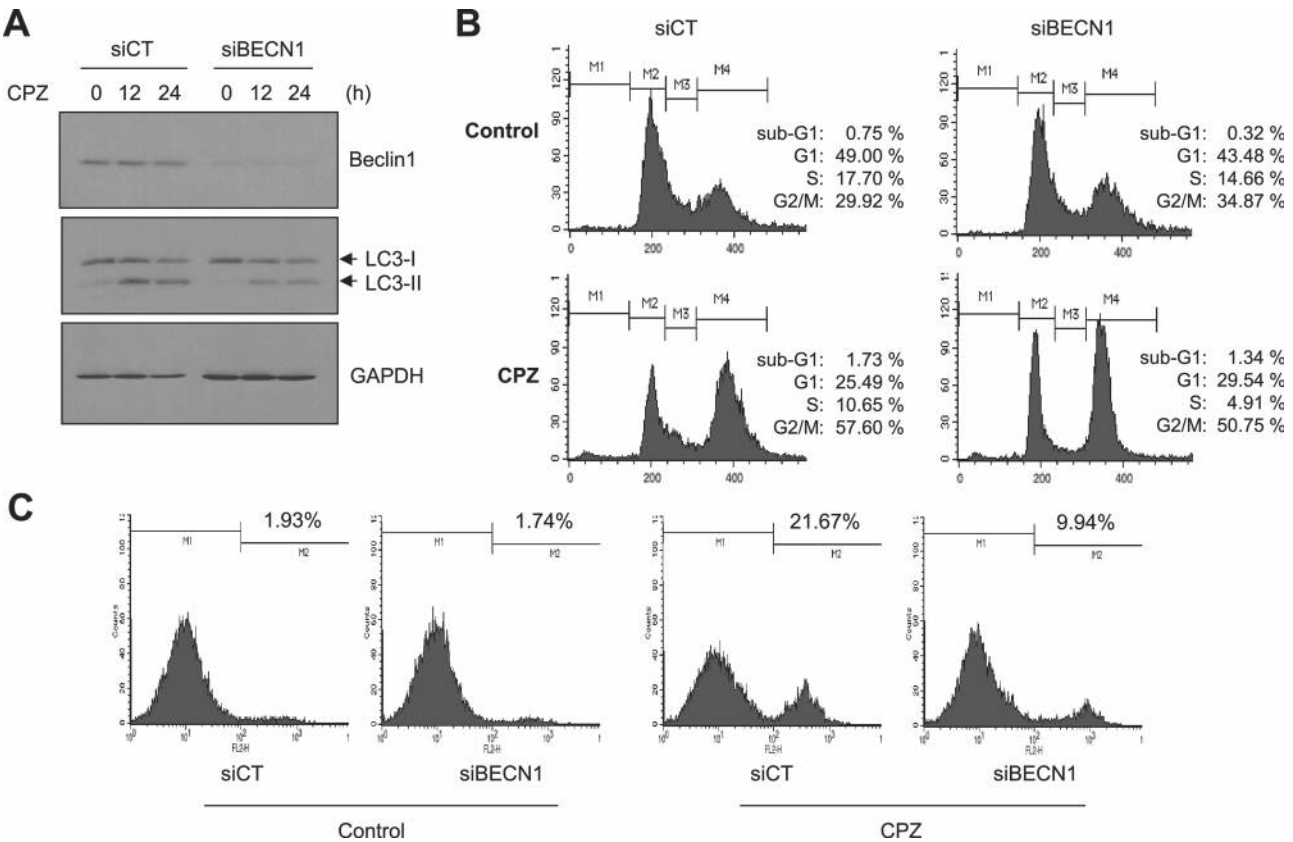

Fig. 4. Effect of Beclin 1 knockdown on CPZ-induced cell death. (**A**) U-87MG cells expressing scrambled control (siCT) or Beclin 1 siRNA (siBECN1) were treated with 20 μM CPZ for different time periods. Whole-cell lysates were prepared and subjected to western blotting using an antibody against Beclin 1 or LC3b. GAPDH antibody was used as an internal control to show equal protein loading. (**B**) Fluorescence-activated cell sorting analysis. U-87MG cells (1×10^5 cells per sample) expressing scrambled control (siCT) or Beclin 1 siRNA (siBECN1) were treated with 20 μM CPZ for 24 h. Cells were harvested, fixed with ethanol and stained with PI. The cellular DNA content was then determined by flow cytometry. M1, sub-G_0/G_1 phase; M2, G_0/G_1 phase; M3. S phase; M4, G_2/M phase. (**C**) Cell death analysis by PI staining. U-87MG cells expressing scrambled control (siCT) or Beclin 1 siRNA (siBECN1) were treated with 20 μM CPZ for 24 h and then stained with 2.5 μg/ml PI for 5 min; PI-positive cells (dead cells) were assessed by flow cytometry.

Downloaded from https://academic.oup.com/carcin/article/34/9/2080/2463384 by guest on 20 August 2022

Figure 3B, available at *Carcinogenesis* Online) in several cancer cells expressing wild-type PTEN, including rat C6 glioma, human glioma T98G and human MDA-MB-231 breast cancer cells. Thus, it seems likely that CPZ-induced cell death is not selective for glioma cells and PTEN status.

CPZ inhibits mTOR by inhibiting Akt

The Akt/mTOR signaling pathway negatively regulates the induction of autophagy and is constitutively activated due to mutation of PTEN in U-87MG glioma cells. To clarify the signaling pathways responsible for CPZ-induced autophagy in U-87MG cells, we examined the effect of CPZ on the phosphorylated status of Akt and mTOR by western blot analysis. The levels of phosphorylated Akt (Ser473) and its downstream effectors GSK3β (Ser9) and mTOR (Thr2481) notably decreased in a time-dependent manner following CPZ treatment (Figure 5A). The phosphorylation of p70S6K (Thr389), a downstream effector of mTOR, also decreased. These data suggest that CPZ inhibits mTOR through the inhibition of AKT.

To investigate whether inhibition of the Akt/mTOR pathway is involved in CPZ-induced autophagy, U-87MG cells were treated with the PI3K inhibitor LY294002, and accumulation of LC3-II was measured by western blotting. Treatment with LY294002 alone resulted in the promotion of LC3-I conversion to LC3-II and further enhanced CPZ-induced accumulation of LC3-II (Figure 5B). On the contrary, exogenous expression of AKT inhibited CPZ-induced LC3-II formation (Figure 5C) and prevented CPZ-induced inhibition of cell proliferation (Figure 5D). These results suggest that inhibition of the AKT/mTOR pathway may participate to CPZ induction of autophagy in U-87MG glioma cells.

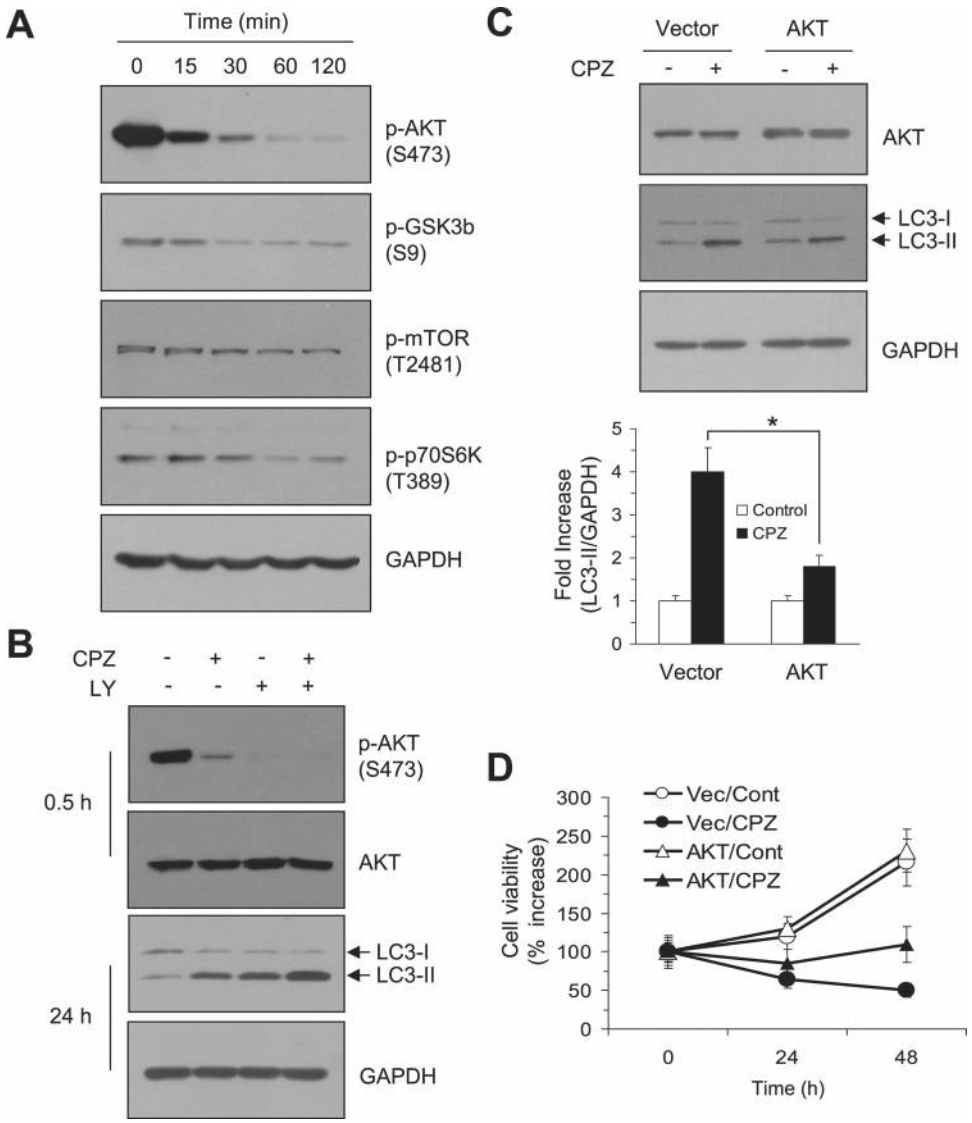

Fig. 5. Effect of Akt inhibition by CPZ on LC3-II formation. (**A**) U-87MG cells were treated with 20 μM CPZ for different time periods (0, 15, 30, 60 or 120 min). Whole-cell lysates were prepared and subjected to western blotting using antibodies against the indicated proteins. GAPDH antibody was used as an internal control to show equal protein loading. (**B**) U-87MG cells were treated with 20 μM CPZ, 25 μM LY294002 (LY) or CPZ plus LY for 0.5 or 24 h, as indicated. Whole-cell lysates were prepared and subjected to western blotting using an antibody against phosphorylated AKT (Ser473) or LC3b, respectively. Akt or GAPDH antibody was used as an internal control to show equal protein loading. (**C**) U-87MG cells were transiently transfected with an expression plasmid for AKT (pSG5/AKT) or empty vector. After 48 h, cells were collected and subjected to western blotting using antibodies against AKT and LC3b. Anti-GAPDH antibodies were used as an internal control to show equal protein loading. The relative band intensity of LC3b-II normalized to GAPDH was determined in three independent experiments by quantitative densitometry (bottom graph). $*P < 0.05$. (**D**) U-87MG cells (1×10^3 cells per sample) transfected with empty vector (Vec) or an expression plasmid for AKT (pSG5/AKT) were treated without (Cont) or with 20 μM CPZ for 24 or 48 h, and cell viability was measured using a Cell Counting Kit-8. The data represent the means ± SD of two independent experiments performed in triplicate.

Downloaded from https://academic.oup.com/carcin/article/34/9/2080/2463384 by guest on 20 August 2022

CPZ inhibits xenograft tumor growth in nude mouse

To determine whether CPZ inhibits tumor growth *in vivo*, U-87MG glioma cells were inoculated subcutaneously into the flanks of athymic nude mice. At 12 days postimplantation, tumor-bearing mice were administered CPZ (20 mg/kg) intraperitoneally once a day. CPZ treatment inhibited xenograft tumor growth on day 24 compared with PBS (control) treatment. Inhibition of tumor growth by CPZ began to be observed after day 17; on day 24, the tumor size of the CPZ-treated group significantly decreased from 690 ± 112 mm^3 in the control group to 390 ± 81 mm^3 in the CPZ-treated group, accounting for a 43.5% inhibition in tumor growth (Figure 6A).

To further evaluate the therapeutic effect of CPZ in the brain, U-87MG cells were implanted into the brain of athymic nude mouse. After 4 days, tumor-bearing mice were administered CPZ intraperitoneally (20 mg/kg/day). CPZ treatment significantly delayed tumor development as revealed by hematoxylin-stained sections (Figure 6B). Immunohistochemical staining revealed LC3 puncta in the tumor tissues that received CPZ (Figure 6C), suggesting the induction of autophagy in xenograft intracranial tumors by CPZ. To further confirm the induction of autophagy *in vivo*, EM analysis was performed. Tumor regions in mice that received CPZ increased the presence of vacuoles (Figure 6D), suggesting that CPZ can achieve effective circulating levels to inhibit tumor growth of brain xenografts through, at least in part, stimulating autophagy *in vivo*.

Discussion

CPZ was first developed as a neuroleptic agent for the control of psychotic symptoms, such as schizophrenia and bipolar disorder. In addition to antipsychotic actions, CPZ exerts antitumor activity in numerous types of cancer (23,24). However, the effect of CPZ on the induction of autophagy has not been studied. In this study, we show that CPZ induces autophagic cell death but not apoptosis through modulation of the Akt/mTOR signaling pathway as well as through inhibition of cell cycle progression in PTEN-null U-87MG glioma cells.

CPZ inhibited tumor cell growth, as revealed by deregulation of cell cycle progression, induction of cell death, inhibition of long-term

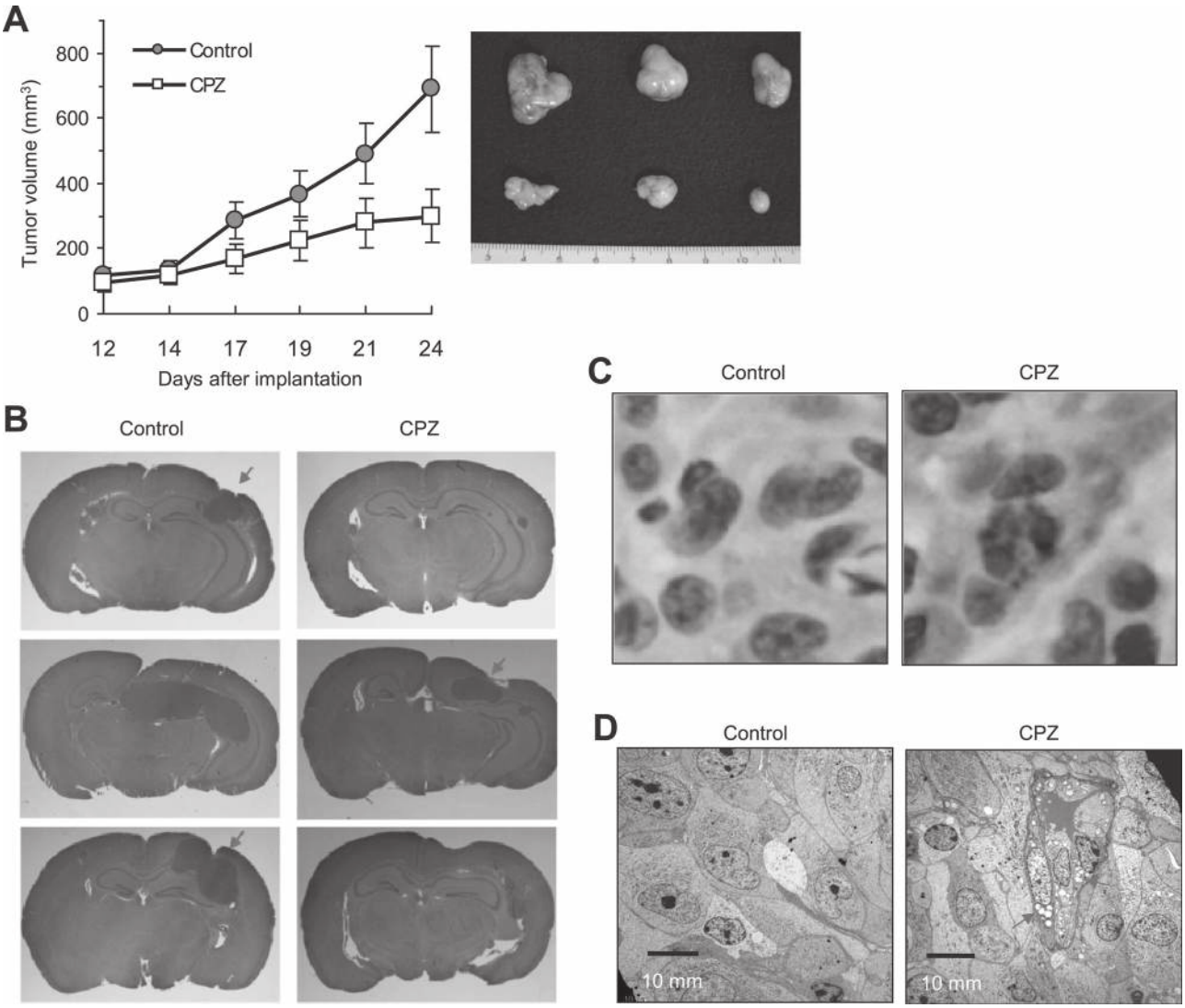

Fig. 6. Inhibitory effect of CPZ on xenograft tumor growth. (**A**) U-87MG cells were injected subcutaneously into the right flank of each nude mouse. After 12 days, mice were administered PBS(control) or CPZ (20 mg/kg) daily. The mean volume of xenograft tumors were measured at intervals of every 2–3 days with calipers. Tumor-possessing nude mice that received PBS or CPZ (20 mg/kg/day) were killed at 24 days postimplantation of U-87MG cells. Right panel shows tumors isolated from nude mice that received PBS or CPZ (20 mg/kg/day). (**B**) Nude mice bearing intracranial U-87MG xenograft tumors were treated with PBS(control) or CPZ (20 mg/kg/day) daily for 7 days. Brain sections were prepared and stained with hematoxylin and eosin. (**C**) Representative photographs of an intracranial U-87MG xenograft tumor stained with LC3b antibodies. **(D)** Representative EM images of U-87MG xenograft brain tumor. Arrows indicate autophagic vacuoles. Bars, 10 μm.

Downloaded from https://academic.oup.com/carcin/article/34/9/2080/2463384 by guest on 20 August 2022

clonogenic survival and inhibition of xenograft intracranial tumor growth *in vivo*. The fluorescence-activated cell sorting analysis of our study showed that CPZ caused a decrease in the population of the G_0/G_1 phase with a concomitant increase in G_2/M phase cells. This result is consistent with a previous report showing that the antiproliferative effects of CPZ is linked to mitotic arrest through inhibition of the motor activity of the mitotic kinesin KSP/Eg5 in HCT116 and A549 cells (25). We also previously reported that CPZ induces cell cycle arrest through induction of p21/Waf1/Cip1 in rat C6 glioma cells (28). Thus, CPZ has the ability to reduce the proliferation of U-87MG cells, presumably by inhibiting cell cycle progression.

Programmed cell death is processed morphologically and is defined as two types; apoptosis (type-I) and autophagic cell death (type-II). Apoptosis is mediated by a cascade of a caspase family activation and leads to cellular shrinkage with chromatin condensation and nuclear fragmentation. Autophagy is mediated by activation of a series of ATG proteins and is characterized by accumulation of acidic vesicular organelles engulfing bulk cytoplasmic organelles such as mitochondria, the Golgi apparatus, polyribosomes and the endoplasmic reticulum. Our results clearly indicate that CPZ triggered cell death in U-87MG glioma cells but had no effect on the occurrence of a sub-G_0/G_1 population of the cell cycle, the presence of PS on the outer cell membranes and the expression of PARP cleavage. Additionally, inhibition of caspases by pan-caspase inhibitor zVAD-fmk treatment did not alter CPZ-induced cell death, suggesting that apoptosis is not involved in CPZ-induced cell death of U-87MG glioma cells. We further examined whether autophagy is involved in CPZ-induced cell death in U-87MG cells. Our data demonstrated that CPZ significantly increased the vacuoles in the cytoplasm as revealed by EM analysis. We also found the presence of the punctated form of LC3 in CPZ-treated U-87MG cells. Time course experiments revealed detectable increases in the levels of LC3-II within 6h of CPZ exposure. Knockdown of Beclin 1 by siRNA in U-87MG cells prevented CPZ-induced LC3-II accumulation. Thus, CPZ induces autophagy through Beclin 1-dependent pathway. Furthermore, knockdown of Beclin 1 resulted in blockade of CPZ-induced cell death. Numerous reports have demonstrated that autophagy can be induced in cancer cells that are resistant to radiotherapy and chemotherapy. Thus, although accurate molecular hallmarks and methods for measuring autophagic cell death specifically have not been established until now, we conclude that autophagy contributes to CPZ-induced cell death in U-87MG glioma cells.

PTEN is a tumor suppressor that modulates cell growth and survival by inhibiting the PI3K/Akt pathway. It also plays a role in enhancing autophagy. In fact, overexpression of PTEN prevents interleukin 13-induced suppression of autophagy in colon cancer cells (17). In U-87MG glioma cells, PTEN is not functional due to a frameshift mutation (16,37), resulting in the constitutive activation of the PI3K signaling pathway. mTOR is a member of the PI3K-related kinase family, which is involved in growth regulation, proliferation and cell metabolism (38). mTOR is a downstream effector of the PI3K/Akt signaling pathway. PTEN enhances autophagy (17), whereas Akt/mTOR inhibits autophagy through phosphorylation of Atg13, a component of the autophagy-initiating kinase Atg1 complex, which is involved in the activation of Vps34, a class III PI3K (18). This study demonstrated that CPZ inhibited mTOR by inhibiting Akt in U-87MG glioma cells. Indeed, inhibition of PI3K by LY294002 treatment alone induced accumulation of LC3-II, and combined treatment with CPZ and LY294002 more potently enhanced LC3-II formation, whereas exogenous expression of AKT partially prevented CPZ-induced autophagy and cell death. However, the mechanism by which CPZ modulates AKT remains unknown.

Phenothiazines, such as CPZ, are strong CaM antagonist (39). CaM is a ubiquitous intracellular Ca^{2+} receptor (40), and Ca^{2+}-bound CaM (Ca^{2+}/CaM) targets many proteins that are involved in Ca^{2+}-mediated regulation of gene expression and regulation of cellular proliferation processes, including cell cycle progression (41,42). Ca^{2+}/CaM is also directly bound to the p110γ subunit of PI3K and plays a critical role in the activation of Akt and cell proliferation in diverse cell types (43,44). Furthermore, Ca^{2+}/CaM is associated with neurotrophin-induced activation of Akt, whereas abolition of intracellular Ca^{2+} or CaM inhibits Akt activation (44–46). Akt is also phosphorylated and activated by Ca^{2+}/CaM-dependent protein kinase kinase through a PI3K-independent pathway, which in turn phosphorylates Bcl-2 antagonist of cell death (BAD) and protects NG108 cells from serum withdrawal-induced apoptosis (47), implicating the role of Ca^{2+}/CaM in activation of Akt via PI3K-dependent and PI3K-independent pathways. Furthermore, inhibition of CaM-dependent protein kinase kinase or CaM-dependent protein kinase reduced starvation-induced autophagy (48). These results raise the possibility that CPZ could inhibit Akt phosphorylation through the inhibition of Ca^{2+}/CaM signaling to release mTOR inhibition of autophagy. Indeed, we also found that other structurally unrelated CaM antagonists, such as W-7 and W-13, could induce LC3-II formation in U-87MG cells (Supplementary Figure 4, available at *Carcinogenesis* Online).

Beclin 1 has been found to be a Bcl-2-interacting protein that contains a Bcl-2-homology-3 (BH3) domain. Beclin 1 also interacts with the class III PI3K family and plays a central role in regulating autophagy (34,36). The human *Beclin 1* gene is localized to chromosome 17q21, a tumor-susceptibility locus that is deleted in up to 75% of ovarian cancers (49), 50% of breast cancers (50) and 40% of prostate cancers (51). Allelic deletion of the *Beclin 1* gene was found in 41% of tested breast cancer cell lines (52). In normal breast epithelial cells, Beclin 1 is ubiquitously expressed but is frequently low or undetectable in malignant breast epithelial cells, suggesting that decreased expression of Beclin 1 may be important in breast cancer development (34). In glioblastoma cells, Beclin 1 protein levels are often reduced during gliomagenesis (53) and high levels of Beclin 1 expression are positively correlated with high prognosis (54). Our study clearly showed that silencing of Beclin 1 by siRNA blocked CPZ-induced cell death, which provided further evidence to support the role of Beclin 1 in antitumor activity in PTEN-deleted human malignant glioma.

In conclusion, this study demonstrated that the antipsychotic agent CPZ triggers apoptosis-independent autophagic cell death in PTEN-null U-87MG glioma cells. Given that CPZ is widely available and can readily cross the blood–brain barrier and accumulate in the brain, the results of our study may help to promote the potential use of the CPZ as a therapeutic supplement for PTEN-mutated human gliomas.

Supplementary material

Supplementary Figures 1–4 can be found at http://carcin.oxfordjournals.org/

Funding

Korea Healthcare Technology R&D Project, the Ministry for Health & Welfare (A101915 to S.Y.S.); the Mid-career Researcher Program through National Research Foundation grant funded by the Ministry of Science, ICT and Future Planning (2012-0005025 to S.Y.S., 2012-013311 to Y.H.L.).

Acknowledgement

This article was supported by the KU Research Professor Program of Konkuk University.

Conflict of Interest Statement: None declared.

References

1. Levine,B. *et al.* (2004) Development by self-digestion: molecular mechanisms and biological functions of autophagy. *Dev. Cell*, **6**, 463–477.
2. Boya,P. *et al.* (2005) Inhibition of macroautophagy triggers apoptosis. *Mol. Cell. Biol.*, **25**, 1025–1040.
3. Gills,J.J. *et al.* (2007) Nelfinavir, A lead HIV protease inhibitor, is a broad-spectrum, anticancer agent that induces endoplasmic reticulum stress,

Downloaded from https://academic.oup.com/carcin/article/34/9/2080/2463384 by guest on 20 August 2022

autophagy, and apoptosis *in vitro* and *in vivo*. *Clin. Cancer Res*., **13**, 5183–5194.
4. Kuo,P.L. *et al.* (2006) Plumbagin induces G2-M arrest and autophagy by inhibiting the AKT/mammalian target of rapamycin pathway in breast cancer cells. *Mol. Cancer Ther*., **5**, 3209–3221.
5. Baehrecke,E.H. (2005) Autophagy: dual roles in life and death? *Nat. Rev. Mol. Cell Biol*., **6**, 505–510.
6. Kanzawa,T. *et al.* (2004) Role of autophagy in temozolomide-induced cytotoxicity for malignant glioma cells. *Cell Death Differ*., **11**, 448–457.
7. Tiwari,M. *et al.* (2008) Inhibition of N-(4-hydroxyphenyl)retinamide-induced autophagy at a lower dose enhances cell death in malignant glioma cells. *Carcinogenesis*, **29**, 600–609.
8. Shingu,T. *et al.* (2009) Inhibition of autophagy at a late stage enhances imatinib-induced cytotoxicity in human malignant glioma cells. *Int. J. Cancer*, **124**, 1060–1071.
9. Lomonaco,S.L. *et al.* (2009) The induction of autophagy by gamma-radiation contributes to the radioresistance of glioma stem cells. *Int. J. Cancer*, **125**, 717–722.
10. Liu,W.T. *et al.* (2011) Minocycline inhibits the growth of glioma by inducing autophagy. *Autophagy*, **7**, 166–175.
11. Alonso,M.M. *et al.* (2008) Delta-24-RGD in combination with RAD001 induces enhanced anti-glioma effect via autophagic cell death. *Mol. Ther*., **16**, 487–493.
12. Chao,A.C. *et al.* (2011) α-Mangostin, a dietary xanthone, induces autophagic cell death by activating the AMP-activated protein kinase pathway in glioblastoma cells. *J. Agric. Food Chem*., **59**, 2086–2096.
13. Aoki,H., *et al.* (2007) Evidence that curcumin suppresses the growth of malignant gliomas in vitro and in vivo through induction of autophagy: role of Akt and ERK signaling pathways. *Mol Pharmacol.*, **72**, 29–39.
14. Sekulić,A. *et al.* (2000) A direct linkage between the phosphoinositide 3-kinase-AKT signaling pathway and the mammalian target of rapamycin in mitogen-stimulated and transformed cells. *Cancer Res*., **60**, 3504–3513.
15. Altomare,D.A. *et al.* (2005) Perturbations of the AKT signaling pathway in human cancer. *Oncogene*, **24**, 7455–7464.
16. Steck,P.A. *et al.* (1997) Identification of a candidate tumour suppressor gene, MMAC1, at chromosome 10q23.3 that is mutated in multiple advanced cancers. *Nat. Genet*., **15**, 356–362.
17. Arico,S. *et al.* (2001) The tumor suppressor PTEN positively regulates macroautophagy by inhibiting the phosphatidylinositol 3-kinase/protein kinase B pathway. *J. Biol. Chem*., **276**, 35243–35246.
18. Petiot,A. *et al.* (2000) Distinct classes of phosphatidylinositol 3'-kinases are involved in signaling pathways that control macroautophagy in HT-29 cells. *J. Biol. Chem*., **275**, 992–998.
19. Takeuchi,H. *et al.* (2005) Synergistic augmentation of rapamycin-induced autophagy in malignant glioma cells by phosphatidylinositol 3-kinase/protein kinase B inhibitors. *Cancer Res*., **65**, 3336–3346.
20. Snyder,S.H. *et al.* (1974) Drugs, neurotransmitters, and schizophrenia. *Science*, **184**, 1243–1253.
21. Zarnowska,E.D. *et al.* (2001) Differential effects of chlorpromazine on ionotropic glutamate receptors in cultured rat hippocampal neurons. *Neurosci. Lett*., **305**, 53–56.
22. Eisenberg,S. *et al.* (2008) Differential interference of chlorpromazine with the membrane interactions of oncogenic K-Ras and its effects on cell growth. *J. Biol. Chem*., **283**, 27279–27288.
23. Nordenberg,J. *et al.* (1999) Effects of psychotropic drugs on cell proliferation and differentiation. *Biochem. Pharmacol*., **58**, 1229–1236.
24. Zhelev,Z. *et al.* (2004) Phenothiazines suppress proliferation and induce apoptosis in cultured leukemic cells without any influence on the viability of normal lymphocytes. Phenothiazines and leukemia. *Cancer Chemother. Pharmacol*., **53**, 267–275.
25. Lee,M.S. *et al.* (2007) The novel combination of chlorpromazine and pentamidine exerts synergistic antiproliferative effects through dual mitotic action. *Cancer Res*., **67**, 11359–11367.
26. Choi,J.H. *et al.* (2008) Potential inhibition of PDK1/Akt signaling by phenothiazines suppresses cancer cell proliferation and survival. *Ann. N. Y. Acad. Sci*., **1138**, 393–403.
27. Franken,N.A. *et al.* (2006) Clonogenic assay of cells *in vitro*. *Nat. Protoc*., **1**, 2315–2319.
28. Shin,S.Y. *et al.* (2010) Chlorpromazine activates p21Waf1/Cip1 gene transcription via early growth response-1 (Egr-1) in C6 glioma cells. *Exp. Mol. Med*., **42**, 395–405.
29. Shin,S.Y. *et al.* (2011) 5-Methoxyflavanone induces cell cycle arrest at the G2/M phase, apoptosis and autophagy in HCT116 human colon cancer cells. *Toxicol. Appl. Pharmacol*., **254**, 288–298.
30. Ito,H. *et al.* (2006) Autophagic cell death of malignant glioma cells induced by a conditionally replicating adenovirus. *J. Natl Cancer Inst*., **98**, 625–636.
31. Lum,J.J. *et al.* (2005) Growth factor regulation of autophagy and cell survival in the absence of apoptosis. *Cell*, **120**, 237–248.
32. Kirisako,T. *et al.* (1999) Formation process of autophagosome is traced with Apg8/Aut7p in yeast. *J. Cell Biol*., **147**, 435–446.
33. Kabeya,Y. *et al.* (2000) LC3, a mammalian homologue of yeast Apg8p, is localized in autophagosome membranes after processing. *EMBO J*., **19**, 5720–5728.
34. Liang,X.H. *et al.* (1999) Induction of autophagy and inhibition of tumorigenesis by beclin 1. *Nature*, **402**, 672–676.
35. Kerr,R.A. (2006) Ocean science. Creatures great and small are stirring the ocean. *Science*, **313**, 1717.
36. Kihara,A. *et al.* (2001) Beclin-phosphatidylinositol 3-kinase complex functions at the trans-Golgi network. *EMBO Rep*., **2**, 330–335.
37. Li,J. *et al.* (1997) PTEN, a putative protein tyrosine phosphatase gene mutated in human brain, breast, and prostate cancer. *Science*, **275**, 1943–1947.
38. Rosner,M. *et al.* (2008) The mTOR pathway and its role in human genetic diseases. *Mutat. Res*., **659**, 284–292.
39. Prozialeck,W.C. *et al.* (1982) Inhibition of calmodulin by phenothiazines and related drugs: structure-activity relationships. *J. Pharmacol. Exp. Ther*., **222**, 509–516.
40. Cheung,W.Y. (1980) Calmodulin plays a pivotal role in cellular regulation. *Science*, **207**, 19–27.
41. Santella,L. (1998) The role of calcium in the cell cycle: facts and hypotheses. *Biochem. Biophys. Res. Commun*., **244**, 317–324.
42. Kahl,C.R. *et al.* (2003) Regulation of cell cycle progression by calcium/calmodulin-dependent pathways. *Endocr. Rev*., **24**, 719–736.
43. Fischer,R. *et al.* (1998) High affinity calmodulin target sequence in the signalling molecule PI 3-kinase. *FEBS Lett*., **425**, 175–177.
44. Pérez-García,M.J. *et al.* (2004) Glial cell line-derived neurotrophic factor increases intracellular calcium concentration. Role of calcium/calmodulin in the activation of the phosphatidylinositol 3-kinase pathway. *J. Biol. Chem*., **279**, 6132–6142.
45. Egea,J. *et al.* (2001) Neuronal survival induced by neurotrophins requires calmodulin. *J. Cell Biol*., **154**, 585–597.
46. Cheng,A. *et al.* (2003) Calmodulin mediates brain-derived neurotrophic factor cell survival signaling upstream of Akt kinase in embryonic neocortical neurons. *J. Biol. Chem*., **278**, 7591–7599.
47. Yano,S. *et al.* (1998) Calcium promotes cell survival through CaM-K kinase activation of the protein-kinase-B pathway. *Nature*, **396**, 584–587.
48. Pfisterer,S.G. *et al.* (2011) Ca2+/calmodulin-dependent kinase (CaMK) signaling via CaMKI and AMP-activated protein kinase contributes to the regulation of WIPI-1 at the onset of autophagy. *Mol. Pharmacol*., **80**, 1066–1075.
49. Russell,S.E. *et al.* (1990) Allele loss from chromosome 17 in ovarian cancer. *Oncogene*, **5**, 1581–1583.
50. Futreal,P.A. *et al.* (1992) Detection of frequent allelic loss on proximal chromosome 17q in sporadic breast carcinoma using microsatellite length polymorphisms. *Cancer Res*., **52**, 2624–2627.
51. Gao,X. *et al.* (1995) Loss of heterozygosity of the BRCA1 and other loci on chromosome 17q in human prostate cancer. *Cancer Res*., **55**, 1002–1005.
52. Aita,V.M. *et al.* (1999) Cloning and genomic organization of beclin 1, a candidate tumor suppressor gene on chromosome 17q21. *Genomics*, **59**, 59–65.
53. Miracco,C. *et al.* (2007) Protein and mRNA expression of autophagy gene Beclin 1 in human brain tumours. *Int. J. Oncol*., **30**, 429–436.
54. Pirtoli,L. *et al.* (2009) The prognostic role of Beclin 1 protein expression in high-grade gliomas. *Autophagy*, **5**, 930–936.

Received November 15, 2012; revised May 7, 2013; accepted May 13, 2013

Downloaded from https://academic.oup.com/carcin/article/34/9/2080/2463384 by guest on 20 August 2022